

Priority Index to Distribute Power More Fairly During Energy Crises Program

Gabriel V. S. Thé
FEUP, UPorto
Porto, Portugal
up201800712@edu.fe.up.pt

A. Selim Türkoglu
SYSTEC-ARISE,
FEUP, UPorto
Porto, Portugal
asturkoglu@fe.up.pt

Sérgio F. Santos
C-MAST,
UBI
Covilha, Portugal
sfs@ubi.pt

Ozan Erdiñç
SYSTEC-ARISE,
Porto, Portugal
YTU, İstanbul, Türkiye
ozanerding@gmail.com

João P. S. Catalão
SYSTEC-ARISE,
FEUP, UPorto
Porto, Portugal
catalao@fe.up.pt

Abstract—This paper introduces a priority index that blends both socio-economic and technical factors to help distribute power more fairly during energy crises. By considering indicators such as household income, unemployment rates, and building conditions, the model ensures that vulnerable communities receive critical energy services first. Formulated as a mixed-integer quadratically constrained programming problem, it is tested on the CIGRE Low Voltage Test System using real demand and solar generation data. The results show how combining grid power, PV outputs, and stored energy according to each consumer’s priority score can maintain equity and resilience, even when supply is severely limited. These insights offer practical guidance for policymakers and grid operators seeking to protect essential loads and minimize the impact on those most in need.

Index Terms—demand response, distribution system, energy vulnerability, energy fairness, resiliency.

I. INTRODUCTION

The global energy crisis highlights the need for resilient systems, with socio-oriented solutions to enhance flexibility and security. IEA notes that current disruptions are accelerating investment in low-carbon infrastructures to reduce reliance on conventional fuels [1]. However, rising energy costs underscore socio-economic disparities, making energy fairness critical for inclusive growth, especially in vulnerable regions, as emphasized by the World Bank [2]. Distributed generation (DG) and energy storage systems (ESSs) are pivotal in stabilizing energy markets as renewables expand. Additionally, the OECD stresses equitable energy policies to prevent deepening social inequalities, reinforcing the need for fair resource distribution during crises [3].

Energy poverty (EP) can be broadly defined as a condition in which a household cannot achieve and maintain the necessary levels of energy services at home [4]. According to the European Commission, “Energy poverty occurs when a household must reduce its energy consumption to a degree that negatively impacts the inhabitants’ health and well-being”. EP is commonly defined as a multidimensional problem, with complex underlying roots that, however, can be traced back to three main drivers: a) Low income; b) The high proportion of household expenses on energy services; c) Low energy performance of buildings and appliances.

These three drivers are directly correlated. Low income can be associated with energy poverty. Being poor, in the financial sense, translates into low purchasing power for the most basic of services – including energy. Low income can result from low salaries, unemployment, or even more structural societal problems, such as uneven wealth distribution and social exclusion. Furthermore, low-income households have fewer options for better housing and often settle for older and precarious homes.

Low-quality housing, lack of resources to perform renovations, and modern energy-efficient appliances can increase energy bills to an unsustainable expense in the household monthly balance, as low energy efficiency in buildings and appliances is certain to increase total energy consumption. In fact, in some countries, legislation regarding energy efficiency has gained significant attention. The European Union’s Energy Efficiency Directive establishes the principle “Energy Efficiency First”, as it helps reduce overall energy consumption while enhancing energy security and affordability [5].

X. Mei and B.K. Seo sums up the interaction between the previously mentioned factors and health outcomes: “The energy bills squeeze health expenditures, forcing occupants to forgo necessary medication and healthcare treatments. Low-income households tend to be stuck with poor housing quality that causes inadequate indoor air quality and thermal discomfort and have difficulties in affording energy and housing renovation and maintenance costs, which affect psychological stress and threats to well-being” [6].

Energy poverty and vulnerability are critical issues in the global energy transition due to their socio-economic impact, especially on disadvantaged populations. Various studies address these topics by proposing methods, highlighting socio-economic consequences, and suggesting mitigation strategies. For instance, Huang et al. (2021) developed an energy hub model to assess the reliability and vulnerability of multi-energy systems, underscoring the need for integrated energy sources to bolster system resilience [7]. Focusing on geographically challenged areas, Katsoulakos et al. (2014) explored energy poverty in mountainous regions, linking it to economic hardships and advocating for targeted socio-economic and infrastructural interventions [8].

A.S. Türkoglu and J.P.S. Catalão acknowledge the support by the EU Horizon Europe Programme under GA ID: 101160614 (EU-DREAM Project, DOI: 10.3030/101160614). S.F. Santos acknowledges the support by FCT through UIDB/00151/2020 (<https://doi.org/10.54499/UIDB/00151/2020>) and UIDP/00151/2020 (<https://doi.org/10.54499/UIDP/00151/2020>), C-MAST. O. Erdiñç acknowledges the support by FCT through the VESPER project, (<https://doi.org/10.54499/2023.08645.CEECIND/CP2834/CT0007>), and also acknowledges the Young Scientists Award Program (BAGEP) of Science Academy, and the TÜBİTAK 100th year Science Encouragement Award.

In [9], an equitable energy-sharing model is formulated to address energy poverty through peer-to-peer shareholding of distributed photovoltaic resources. The coordinated scheme maximizes user profits and improves overall PV utilization, yet it primarily focuses on local hardware and market-driven exchanges without a broader prioritization framework during crises. A new insurance-based price discovery mechanism is introduced in [10], where blockchain facilitates premium transactions and fuzzy logic assigns a criticality score for cost-effective energy distribution. This approach improves resilience through integrated risk management procedures but does not explicitly incorporate an equitable resource allocation strategy in distribution networks under emergency conditions. In [11], a robust normalized mixed-norm adaptive controller is developed for power quality enhancement in remote wind-solar PV–battery systems. The method mitigates harmonic distortions, improves voltage profiles at the PCC, and ensures stability, though it does not address allocation fairness among competing loads when resources are limited. About the real-world applications; UK Power Networks provides a specialized Priority Services program aimed at supporting vulnerable customers during outages. This initiative includes a dedicated 24-hour contact line, proactive text and voice messaging about power cut statuses or severe weather, and on-site community welfare services such as hot meals, Wi-Fi access, and charge points. In certain critical circumstances, the company also offers free overnight hotel stays and transportation to ensure individuals receive essential care and protection [12].

Building on these efforts, this work proposes an integrated framework that addresses the pressing challenges of energy poverty and equity in power systems during crises by introducing novel indices and restoration strategies. The main contributions of this study are:

- A Priority Index is introduced to quantify socioeconomic and technical vulnerabilities while providing a systematic metric for prioritizing critical loads.
- A priority index-based resource allocation model is developed to enable efficient restoration of critical loads during energy crises.
- Equity is examined by sequentially integrating PV systems and ESS for wealthier customers, thereby facilitating the assessment of energy fairness.

II. METHODOLOGY

In this chapter, the equations used for the present work are demonstrated and described. The model implemented a power network that aimed to minimize the difference between the power demand from the load buses and the actual power the network was able to fulfill. Additionally, the Priority Index also presented the reasoning behind its creation.

A. Priority Index

The Priority Index was heavily inspired by [13]. The paper proposed a novel Energy Poverty Vulnerability Index (EPVI) focused on space heating and cooling needs, which helped identify geographic regions to focus resources and action in energy poverty mitigation. Initially tested for all 3092 civil parishes of Portugal, the method could potentially be replicated across Europe.

The EPVI was composed of two sub-indexes: Energy Gap for H&C (EPG) and Ability to Implement Alleviation Measures (AIAM). The latter took into account socioeconomic indicators, which was an important aspect of the equity-oriented nature of the present work. In this manner, the EP Index developed in this work to perform the load prioritization was mirrored in the AIAM sub-index, to be described in more detail below. To build the AIAM sub-index, the authors conducted a review to identify socioeconomic variables that could quantify a population's ability to implement thermal comfort alleviation or mitigate energy poverty, coming down to 7 final indicators. These indicators were segmented into five intervals of values according to their distribution within Portugal, creating a classification between 1 (minimum ability) and 5 (maximum ability). Finally, a survey was conducted with specialists to classify each indicator's importance, creating a weight for each indicator to highlight its importance to the final AIAM sub-index score. The related weights can be seen in Table I.

In the index, each indicator was valued from 1 to 5 and then multiplied by its respective weight. The 7 weighted indicators were then summed and standardized. To build the Priority Index (ρ) to be used in the current work, an "EP Index" was developed mirroring the characteristics of the previously described AIAM sub-index. A Python code generated random values for each of the 7 indicators between 1 and 5, which were then weighted and summed, creating 10 priority indexes. Those would later be assigned to the 10 load buses in the system, to be described in more detail in the next chapter. Therefore, the formulation for the EP Index for each bus i is:

$$EP\ Index_i = \sum_{N=1}^7 Indicator_{N,i} \cdot Weight_{N,i} \quad (1)$$

B. Mathematical Model

The single objective function is presented in (2). For each load bus i , the difference between the demand and the fulfilled power is minimized, aiming to fulfill as much as possible. The bus is affected by the priority index. ρ_i , to be described in more detail in the next section of this chapter. A higher ρ_i value indicates a higher priority and signals the network where more resources should be allocated.

$$\min \sum_i \sum_t \rho_i \cdot (P_{i,t}^{demand} - P_{i,t}^{fulfilled}) \quad (2)$$

Equation (3) implements the power flow for all buses. The active and reactive power arriving at the bus minus the active and reactive power leaving the bus must be equal to the demand of that bus, plus any losses involved in the lines connected to it.

$$\begin{aligned} P|Q_{i,t}^{gen} + P|Q_{i,t}^{PVinj} + \sum P|Q_{j,i,t}^{flow} - \sum P|Q_{i,j,t}^{flow} \\ = P|Q_{i,j,t}^{loss} + P|Q_{i,t}^{grid,consumed} \end{aligned} \quad (3)$$

TABLE I. INDICATORS AND WEIGHTS OF AIAM SUB-INDEX

N	Socioeconomic Indicator	Weight
1	Population with 4 or fewer years of age (%)	0.44
2	Population with 65 or more years of age (%)	0.67
3	Average monthly income (€)	0.59
4	Dwelling owned by the occupant (%)	0.27
5	Population with a university degree (%)	0.67
6	Unemployment (%)	0.97
7	Building State of Conservation (qualitative)	0.39

The previously mentioned power losses are implemented through (4), which are determined by the resistance and reactance values of the lines connecting the buses and the active and reactive power flowing through them.

$$P|Q_{i,j,t}^{loss} = R|X_{i,j} \cdot [(P_{i,j,t}^{flow})^2 + (Q_{i,j,t}^{flow})^2]/V_0^2 \quad (4)$$

The voltage drops along the buses are defined by (5), and (6) imposes voltage magnitude limits.

$$V_{j,t}^{bus} = V_{i,t}^{bus} - (R_{i,j} * P_{i,j,t}^f + X_{i,j} * Q_{i,j,t}^f)/V_0 \quad (5)$$

$$V_{i,t}^{min} \leq V_{i,t}^{bus} \leq V_{i,t}^{max} \quad (6)$$

Equation (7) maintains power factor consistency for reactive power demand and reactive fulfilled power. Along with the voltage equations from the previous subsection, this models real-world requirements that ensure grid safety, efficiency, and stability.

$$Q_{i,t}^{demand|fulfilled} = \cos(\varphi) \cdot P_{i,t}^{demand|fulfilled} \quad (7)$$

The ESSs are modeled by the following equations. Equation (8) implements continuity, in which the current storage level is determined by the previous storage level, plus additional energy that was stored, minus energy that was consumed. These ESSs were inspired by solar batteries and store excess PV generation.

$$E_{i,t}^{ESS_level} = E_{i,t-1}^{ESS_level} + \Delta T \cdot P_{i,t}^{ESS_stored} \cdot \eta^{ESS} - \Delta T \cdot P_{i,t}^{ESS_consumed} \cdot \frac{1}{\eta^{ESS}} \quad (8)$$

To prevent simultaneous charging and discharging of the ESSs, equations (9) and (10) are created featuring a binary variable, ensuring mutual exclusivity.

$$P_{i,t}^{ESS_stored} \leq P_i^{ESS_min_rate} \cdot u_{i,t} \quad (9)$$

$$P_{i,t}^{ESS_consumed} \leq P_i^{ESS_max_rate} \cdot (1 - u_{i,t}) \quad (10)$$

Equations (11)-(13) constrain the ESS to operate within reason, and are described as follows:

The energy consumed must not be higher than the current storage level:

$$P_{i,t}^{ESS_consumed} \cdot \Delta T \leq E_{i,t}^{ESS_level} \quad (11)$$

Do not store more energy than what is currently being generated:

$$P_{i,t}^{ESS_stored} \leq P_{i,t}^{PV_generated} \quad (12)$$

The storage level must not violate the minimum and maximum nominal capacity:

$$E_i^{ESS_level,min} \leq E_{i,t}^{ESS_level} \leq E_i^{ESS_level,max} \quad (13)$$

Equation (14) models the household PV panel. It allows the decision variable $P_{i,t}^{fulfilled}$, part of the objective function, to have diversified sources. The fulfillment can be composed of energy delivered by the grid, generated by PV, and discharged by ESS.

$$P_{i,t}^{fulfilled} = P_{i,t}^{grid,consumed} + P_{i,t}^{PV,consumed} + P_{i,t}^{ESS,consumed} \quad (14)$$

Equation (15) models PV operation and defines a destination for the energy generated by the panels that should either be directly consumed, stored for later usage, or curtailed.

$$P_{i,t}^{PV_generated} = P_{i,t}^{PV_consumed} + P_{i,t}^{ESS_stored} + P_{i,t}^{PV_curtailed} \quad (15)$$

Equation (16) ensures that the fulfilled active and reactive power does not exceed demand.

$$P|Q_{i,t}^{fulfilled} \leq P|Q_{i,t}^{demand} \quad (16)$$

Equation (17) ensures that for every bus, regardless of its priority index, a minimum level of fulfillment should be attained.

$$P|Q_{i,t}^{fulfilled} \geq P|Q_{i,t}^{fulfilled,min} \quad (17)$$

Finally, equation (18) implements the maximum generation at the slack bus. The decision variable P^{gen} is multiplied by a constant that caps the generation when set to values smaller than 1, thus allowing the creation of energy crisis scenarios.

$$P_{i,t}^{gen} \leq P_{i,t}^{gen,max} \quad (18)$$

III. TEST AND RESULTS

This chapter aims to introduce the test system and present the technical data, and assumptions used to conduct the studies. In Cases 1 through 3, the generation incoming from the slack bus (Bus-1) was limited to simulate an energy crisis, different solutions for mitigation were implemented and their impact was analyzed. The efficiency of the developed method is evaluated using the Gurobi commercial solver and a Python environment. The optimization model has a 30-minute resolution and 48 time frames.

A. Input Data

To run the simulations, the model network is a standard CIGRE 18-Bus Low-Voltage Test System, which a unifilar diagram can be seen in Fig. 1. The main characteristics of the system are; 18 total buses, 10 residential load buses, nominal voltage of 1.05 p.u., minimum voltage 0.9 p.u., maximum voltage 1.1 p.u., power factor ($\cos(\varphi)$) 0.97.

The dataset for demands in this work was extracted from OpenSynth [14], an LF Energy project that allowed users in the United Kingdom to generate synthetic data from their residential smart meters. The readings were assigned at random to the 10-load buses. In Table II, the total daily demand for each load bus is presented, as well as its Priority Index.

The PV dataset is generated from renewables.ninja [15], The parameters for the simulation are; Lat: 41°31'50.7"N, Lon: 6°58'17.4"W (random location picked in Portugal), installed capacity 5 kWp, system losses 10%, tilt 30°, azimuth 180°.

TABLE II. TOTAL DEMAND AND ρ OF EACH LOAD BUS

Bus	Total Daily Demand (kWh)	Priority Index
2	24.39	2.24
4	40.36	2.17
6	26.26	2.04
9	34.66	1.67
11	30.85	1.53
13	27.77	1.41
15	30.55	1.38
16	28.49	1.26
17	25.53	1.22
18	46.53	1.00

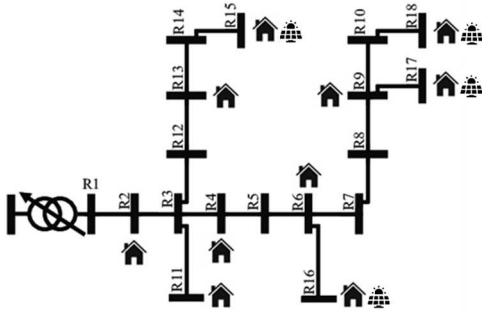


Figure 1. CIGRE 18-Bus Low Voltage Test System.

For a load profile, a random day between January and March was picked. Assuming the same installed capacity and close geographical proximity, the four buses are equipped with the same profile. In Fig. 2, the PV generation curve shows that at 12:00, generation hit its peak of 4 kWh. Total daily PV production relative to each PV-equipped bus (15-18) is 27.71 kWh. The ESSs were implemented as solar batteries, meaning they only store excess energy from PV. From a sample product datasheet, the following parameters are used; usable energy 13.5 kWh, maximum continuous power 5 kW, efficiency 90%.

B. Simulation and Results

To evaluate the efficacy of the proposed model, several case studies were carried out, which are expounded upon below. The test system setup and performance under various constrained energy scenarios are described in detail, with corresponding figures provided in the Appendix.

- Case 1: Generation at the slack bus is capped at 50% max..
- Case 2: Generation at the slack bus is capped at 50% max., and 5 kWp of PV is installed in each designated bus.
- Case 3: Generation at the slack bus is capped at 50% max., and 5 kWp of PV and a 13.5 kWh ESS are installed in each designated bus, beginning on an empty charge.

The fulfillment percentage vs. EP Index is depicted in Fig. 3a for Case-1 illustrates how the equity-based algorithm continues to favor the most disadvantaged buses under tighter supply conditions. As poorer buses, characterized by higher EP Index values, receive sufficient or complete allocations, wealthier buses remain near the established minimum threshold.

While a correlation between EP Index and fulfillment still holds, points for certain mid-priority buses deviate slightly from a purely linear trend. This pattern suggests that the algorithm, though designed to prioritize vulnerable consumers, faces increasing difficulty in fairly distributing limited resources when overall power availability is drastically reduced.

Fig. 4a shows the power deficit by bus, revealing a pattern where buses with lower incomes (and higher EP Index values) experience little to no unmet demand. In contrast, moderate- and high-income buses incur larger deficits, reflecting the allocation routine's decision to protect essential loads first and foremost.

The distribution of points indicates that as the shortage grows more severe, certain mid-tier buses see fluctuating or disproportionately high deficits, suggesting that the algorithm must make harsher trade-offs. Overall, the figure underscores the substantial pressure placed on resource allocation when power shortages are more critical.

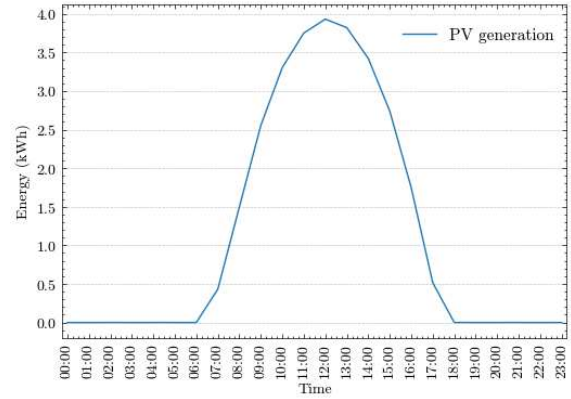


Figure 2. PV generation curve for Buses 15-18.

A detailed comparison of power breakdowns for selected buses is depicted in Fig. 5a, highlighting how the constrained environment affects each socioeconomic segment throughout the day. The poorest bus achieves nearly constant demand fulfillment, maintaining uninterrupted supply in line with its high-priority status. Meanwhile, mid-level buses show partial allocations that fluctuate over time, demonstrating the struggle to secure adequate power once the essential needs of underprivileged users have been accounted for. In contrast, wealthier buses are largely restricted to minimal fulfillment, reinforcing the principle that the routine aims to shield the most vulnerable first when total power is scarce.

The fulfillment percentage vs. EP Index is depicted in Fig. 3b for Case-2 showcases higher overall coverage compared to a strictly grid-dependent scenario under similar generation constraints. Because buses equipped with PV rely less on external supply during daylight hours, more grid power becomes available for non-PV buses. This allocation strategy raises the fulfillment rates of both vulnerable and mid-priority buses. Nevertheless, consumption peaks at night remain a challenge, as solar generation is absent. Fig. 4b presents the power deficit by bus, indicating that although the poorest buses remain a top priority, moderate-priority buses also benefit from reduced shortfalls. PV-equipped buses naturally register fewer deficits during the day, which translates into less strain on the grid and, consequently, smaller deficits for certain non-PV buses as well. However, because nighttime supply still hinges on conventional generation, wealthier buses without PV may face higher unmet demand when solar resources are unavailable.

A power breakdown comparison between selected buses is depicted in Fig. 5b, revealing how PV integration shapes each bus's daily fulfillment profile. High-priority buses remain consistently supplied, while PV-equipped ones enjoy steady coverage whenever sunlight is available. Meanwhile, certain mid-priority buses that rely solely on the grid still endure partial shortages, though these shortages are less severe than in purely grid-dependent scenarios. Ultimately, the figure highlights the importance of diversifying energy sources—particularly in times of constrained generation—and the limitations of relying on solar power alone without energy storage.

The PV breakdown for Bus 18 is illustrated in Fig. 6b, highlighting how solar power supplements its large demand. During sunlit hours, Bus-18 obtains a significant portion of its energy from its own PV panels, thereby relying much less on the limited grid supply. Although this approach alleviates the load on the overall system, it does not fully resolve nighttime deficits. The figure underscores both the advantages of on-site generation during peak daylight hours and the persistent challenge of meeting demand after sunset without storage solutions.

Fig. 3c illustrates how overall load fulfillment behaves in the 50% generation cap scenario for Case-3 when PV systems are combined with energy storage. In the graph, it is evident that buses equipped with PV and ESS enjoy noticeably higher coverage rates than in grid-only arrangements. The energy stored during daylight hours helps bridge evening gaps, which are otherwise hard to meet given the limited grid supply. As a result, the poorest and mid-priority buses can maintain steadier power availability, improving their fulfillment percentages in comparison to scenarios lacking storage solutions.

Fig. 4c focuses on the power deficit distribution across buses, reinforcing the effectiveness of ESS in mitigating shortages. Buses without storage—or with lower priority—still encounter unmet demand, particularly at night when solar generation ceases, but the overall deficit is considerably smaller. The inclusion of ESS for daytime energy capture and evening discharge shifts the curve of deficits downward, indicating fewer and less severe shortfalls for numerous buses. While the strict 50% grid cap continues to pose challenges, these figures confirm that storage can partially offset reduced generation levels.

Fig. 5c shows how the timing of ESS usage impacts individual buses. In this case, the system starts with an empty battery, forcing the bus to rely predominantly on the grid during the early hours. This leads to sharp unmet demand until solar power becomes available to charge the ESS. The early buffer can supply overnight loads, preventing the abrupt drop in fulfillment seen in the empty-battery case. The figure underscores that initial battery status critically affects each bus's ability to ride through periods of low solar production.

How stored solar power is utilized during late-day and evening hours is highlighted in Fig. 6c, when sunlight is no longer present. It provides a broad overview of how surplus PV energy, once it satisfies immediate midday consumption, is diverted into the ESS. Zooming on a specific bus—Bus 18—shows that even a large, high-demand consumer can achieve significantly higher fulfillment by drawing from previously stored energy. However, if the ESS capacity or input from PV remains insufficient, nighttime deficits persist. The figure ultimately stresses the balancing role that storage plays: it helps smooth out supply gaps, yet the grid limit can still leave certain loads partially unserved if overall energy availability is too constrained.

IV. CONCLUSION

This work demonstrated the effectiveness of an equity-focused resource allocation model in safeguarding critical loads during an energy crisis. Under a 50% generation cap, the results showed that the poorest buses benefit most from the priority index: they received near-complete allocations, even as wealthier buses were restricted to minimal thresholds. Integrating PV systems alleviated some of the load on the grid by shifting the daytime supply to PV.

However, nighttime shortfalls persisted when solar generation was unavailable. ESS was also added, and there was a marked decrease in deficits across all consumer groups. Surplus PV power generated during peak sun hours could be stored for evening use, reducing the number and severity of unmet demands, particularly for mid-priority loads. Nonetheless, the system could still encounter constraints if overall grid capacity remained too limited or if battery size was insufficient. Despite these limitations, the approach provided a practical framework for prioritizing vulnerable segments while improving overall network resilience, offering valuable insights to grid operators and policymakers on balancing equity and resource scarcity.

REFERENCES

- [1] International Energy Agency (IEA), "Global Energy Crisis," [Online]. Available: <https://www.iea.org/topics/global-energy-crisis..>
- [2] The World Bank, "Energy Overview," [Online]. Available: <https://www.worldbank.org/en/topic/energy/overview>.
- [3] "Net Zero by 2050" [Online]. Available: https://www.oecd.org/en/publications/net-zero_da477dda-en.html.
- [4] "Energy poverty," Energy. https://energy.ec.europa.eu/topics/markets-and-consumers/energy-consumers-and-prosumers/energy-poverty_en
- [5] "Energy Efficiency Directive," Energy. https://energy.ec.europa.eu/topics/energy-efficiency/energy-efficiency-targets-directive-and-rules/energy-efficiency-directive_en
- [6] X. Mei and B. K. Seo, "The relationships among housing, energy poverty, and health: A scoping review," *Energy Sustainable Development/Energy for Sustainable Development*, vol. 83, p. 101568, Oct. 2024, doi: 10.1016/j.esd.2024.101568.
- [7] W. Huang et al., "Reliability and Vulnerability Assessment of Multi-Energy Systems: an energy hub based method," *IEEE Transactions on Power Systems*, vol. 36, no. 5, pp. 3948–3959, Feb. 2021, doi: 10.1109/tpwrs.2021.3057724.
- [8] N. Katsoulakos, L. Papada, and D. Kaliampakos, "The problem of energy poverty in mountainous areas." 2014, pp. 222–226. doi: 10.1109/iisa.2014.6878794.
- [9] J. Lei et al., "Peer-to-Peer shareholding strategy for distributed photovoltaic systems to curb energy poverty," *IEEE Transactions on Power Systems*, pp. 1–12, Jan. 2024, doi: 10.1109/tpwrs.2024.3506823.
- [10] M. Arora, G. M. Vishwanath, A. Sharma, and N. Chilamkurti, "A novel price discovery insurance scheme for outage resilient energy management system," *IEEE Transactions on Industry Applications*, vol. 60, no. 2, pp. 1986–2001, Dec. 2023, doi: 10.1109/tia.2023.3339471.
- [11] F. Chishti, S. Murshid, and B. Singh, "Robust normalized Mixed-Norm Adaptive Control Scheme for PQ improvement at PCC of a remotely located Wind-Solar PV-BES microgrid," *IEEE Transactions on Industrial Informatics*, vol. 16, no. 3, pp. 1708–1721, Jun. 2019, doi: 10.1109/tii.2019.2923641.
- [12] "Priority Services | UK Power Networks." <https://www.ukpowernetworks.co.uk/power-cut/priority-services>
- [13] J. P. Gouveia, P. Palma, and S. G. Simoes, "Energy poverty vulnerability index: A multidimensional tool to identify hotspots for local action," *Energy Reports*, vol. 5, pp. 187–201, Feb. 2019, doi: 10.1016/j.egy.2018.12.004.
- [14] LF Energy, "OpenSynth - LF Energy," LF Energy, Jan. 20, 2025. <https://lfenergy.org/projects/opensynth/>
- [15] "Renewables.ninja." <https://www.renewables.ninja/>

APPENDIX

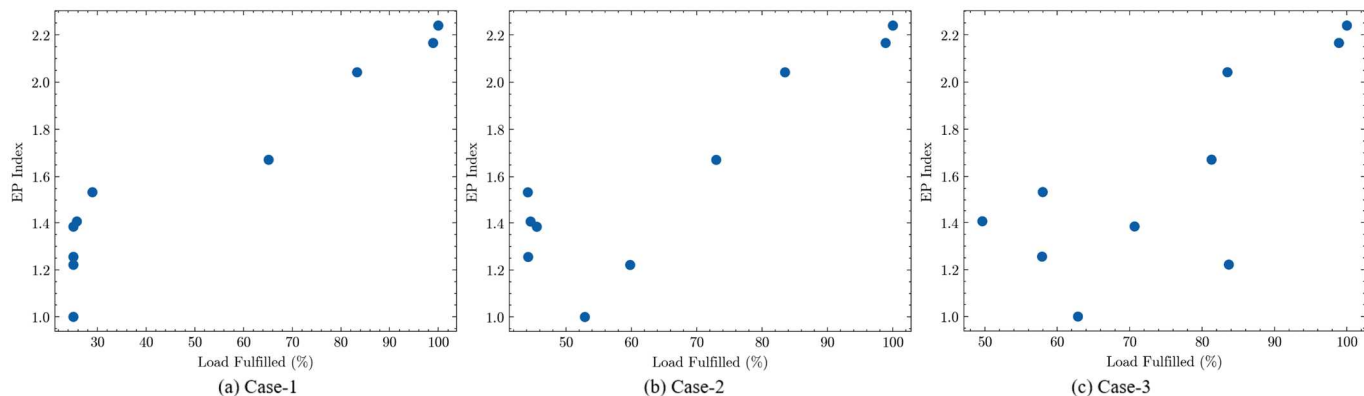


Figure 3. Fulfillment percentage vs. EP Index.

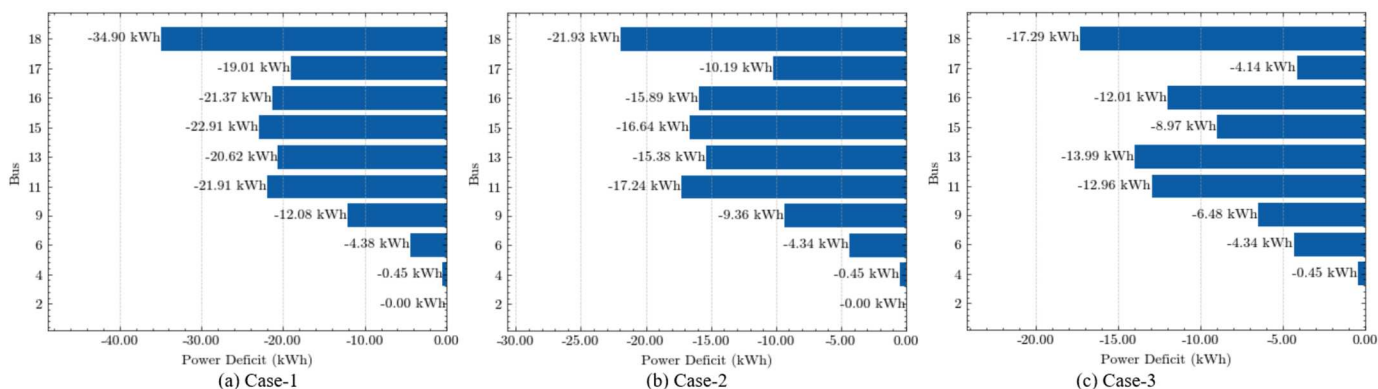
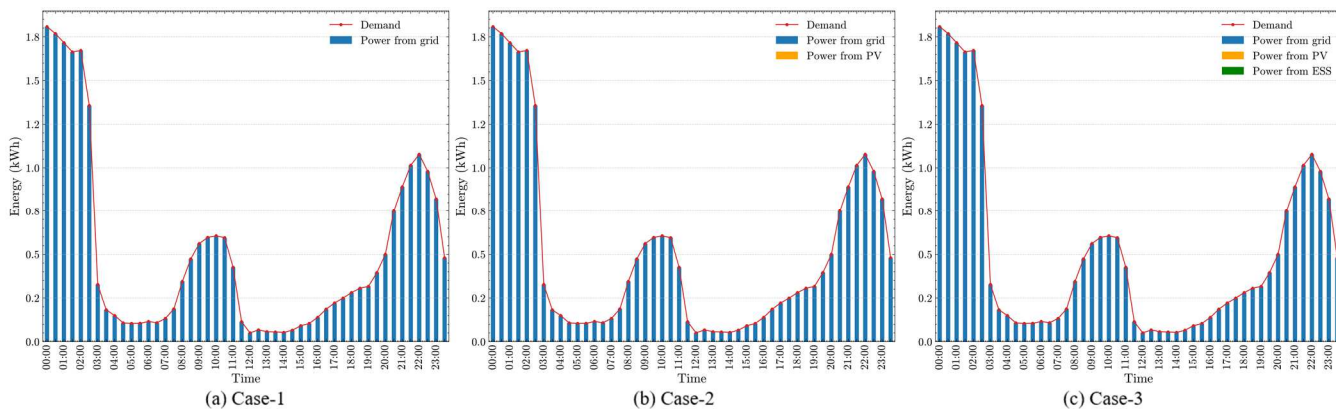
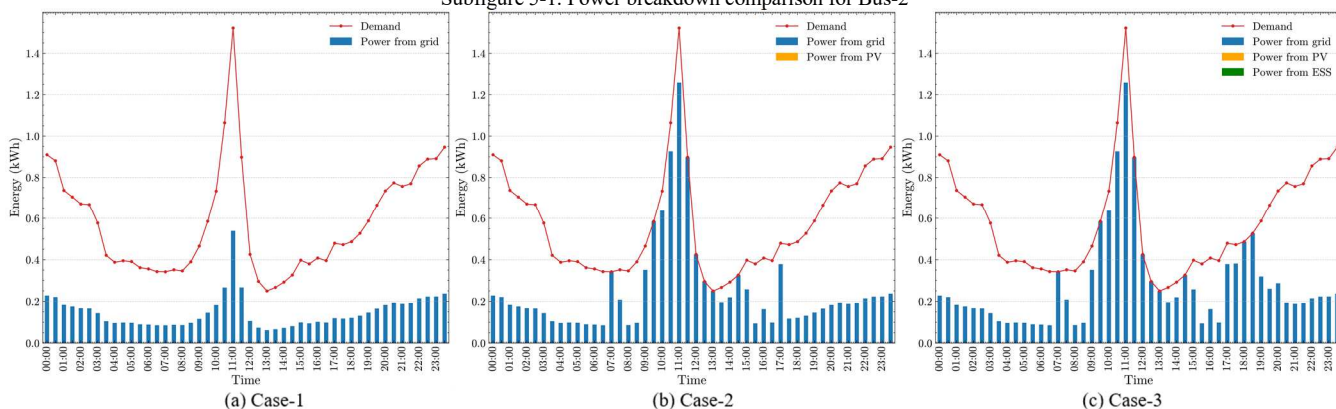


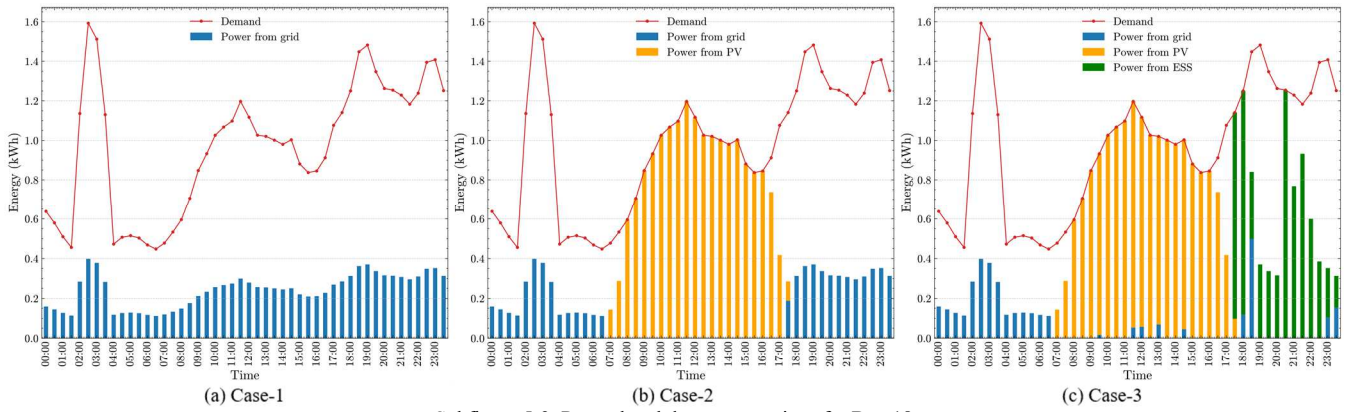
Figure 4. Power deficit by Bus.



Subfigure 5-1. Power breakdown comparison for Bus-2



Subfigure 5-2. Power breakdown comparison for Bus-13



Subfigure 5-3. Power breakdown comparison for Bus-18
 Figure 5. Power breakdown comparison for Bus-2, Bus-13 and Bus-18.

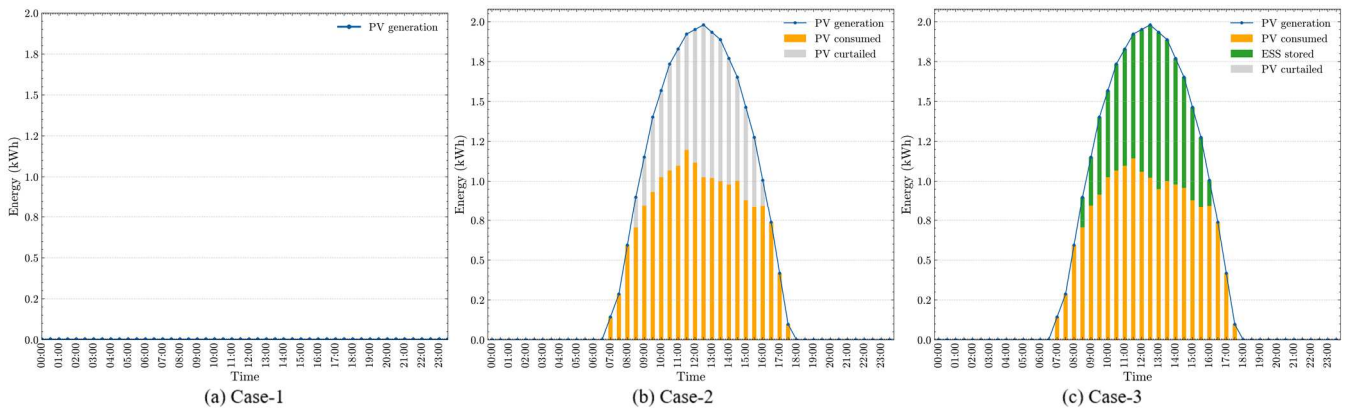


Figure 6. PV breakdown for Bus-18